water

MDPI

Article

Evolution of Water Conveyance Capacity through Hydraulic Transition Processes in Circular Drop Manholes

Chunyue Zhu [1,2,*], Feidong Zheng [3,*], Genhua Yan [1] and Xianrui Shi [1]

[1] Hydraulic Engineering Department, Nanjing Hydraulic Research Institute, No. 225 Guangzhou Road, Nanjing 210029, China; ghyan@nhri.cn (G.Y.); shixianrui56@gmail.com (X.S.)
[2] College of Water Conservancy and Hydropower Engineering, Hohai University, No. 1 Xikang Road, Nanjing 210098, China
[3] College of River and Ocean Engineering, Chongqing Jiaotong University, No. 66 Xuefu Road, Chongqing 400074, China
* Correspondence: zhucy@hhu.edu.cn (C.Z.); feidongzheng@cqjut.edu.cn (F.Z.)

Abstract: Circular drop manholes are widely implemented for steep catchments in urban drainage networks. Poor downstream hydraulic transition processes of a manhole system, i.e., the formation of hydraulic jump near the outlet entrance, and the sudden transition from free surface to pressurized flow with bursts of air in the outflow pipe can severely constraint the capacity of water conveyance. In this paper, we defined four basic hydraulic stages that indicate where hydraulic transition processes begin and end. The measurements of typical manhole models with different drop heights were conducted under different inflow and outflow conditions. Three types of transition processes covering all flow patterns have resulted into a graphical visualization by analyzing two pairs of dimensionless parameters. The flow inside a circular drop manhole was considered to reach its discharge capacity when the abrupt drop of manhole water level is visible in the fully aerated flow pattern. Four empirical equations revealing the water level filling ratio and discharge efficiency at different hydraulic stages were also presented for further predictions of choking risks.

Keywords: transition processes; hydraulics; drop manhole; choking; aerated flow

Citation: Zhu, C.; Zheng, F.; Yan, G.; Shi, X. Evolution of Water Conveyance Capacity through Hydraulic Transition Processes in Circular Drop Manholes. *Water* **2021**, *13*, 2277. https://doi.org/10.3390/w13162277

Academic Editor: Giuseppe Pezzinga

Received: 29 June 2021
Accepted: 18 August 2021
Published: 20 August 2021

1. Introduction

Urban drainage pipes generally follow local surface terrains in plain area. However, when it comes to a steep topography, downstream hydraulic jumps, erosion of the pipe walls and surcharging of the pipe may form inside the conduit due to the exceeding flow velocities. Drop manholes are thus inserted at certain intervals along a pipeline for steep catchments: the storm water or wastewater plunges into a manhole with a fully energy dissipation, then be transported to a lower trunk with safe flow rates. The widely implement of a circular drop manholes can allow control of the longitudinal free-surface profile to minimize possible of downstream conditions [1]. For above reasons, drop manholes have been the standard elements in urban drainage networks.

An ideal manhole design has to take two aspects into account: (1) achieve the adequate energy dissipation to avoid excessive flow velocities and (2) optimize flow conditions to improve the water carrying efficiency of drainage sewers. In terms of the kinetic energy reduction, both the energy loss across the manhole and the residual energy head have been systematically studied with experiments and numerical simulations. On the other hand, poor hydraulic performances caused by complicated transition processes, i.e., the formation of hydraulic jump near the outlet entrance and the sudden transition from free surface to pressurized flow with bursts of air in the outflow pipe, have also been investigated by a detailed classification of flow patterns and dimensionless considerations.

The traditional description of flow patterns inside a drop manhole is from a perspective of the jet impact locations. Chason [2,3] defined three basic flow regimes, named

Regime R1, R2 and R3 for rectangular drop manholes. His classification further extended in the submerged regimes R2 and R3 for circular drop manholes by Granta [4] has become a standard reference for all studies on circular drop manholes about energy dissipations [5,6] and choking occurrences [7,8].This classic classification of flow patterns is detailed organized as:

- In Regime R1, the falling jet plunges directly onto the bottom pool of the manhole;
- Regime R2 can be observed when the jet impacts the manhole outlet zone: Regime R2a if the jet falls in the zone between the manhole bottom and the manhole outlet; Regime R2b if it impacts the downstream sewer invert; Regime R2c if it impacts on the manhole inner sidewall just above the manhole outlet;
- Regime R3 occurs if the falling jet impacts the opposite manhole side wall: Regime R3a if the falling jet keeps a compact core beyond the impact location; Regime R3b if a spiraling flow runs along the manhole wall interfering for high discharges.

On this foundation, Granta [4] characterized hydraulic transitions with the impact number $I = \sqrt{2s/g}\ V_0/D_M$, where s = manhole drop height; D_M = manhole diameter; g = gravity acceleration; and V_0 = approaching flow velocity. His experimental evidence demonstrated that the flow would transfer from Regime R1 to R2 when $I \cong 0.6$; from R2 to R3a when $I \cong 0.95$ to 1; and from R3a to R3b when $I \cong 1.5$. Empirical equations for manhole pool heights and the prediction of air demands under the relative regimes were further proposed [8].

The flow regimes sorted by the impingent locations, however, are not entirely suitable to describe the changes of water conveyance capacity of the manhole system. For a given impact location of a falling jet, the diversities in manhole geometrical characteristics, tailwater pressures and air entrainments may result in vastly different hydraulic properties as well as the various presence of flow discharge downstream the drop manhole. For a very small relative drop ratio of the drop height to the manhole diameter, most flowrate in Regime R2 is conveyed to the outlet pipe directly without tailwater effects. As the tailwater depth increases, the downstream flow changes from a repelled jump in the exit pipe to a jump at the base of the drop manhole, and then to a critical or a submerged jump near the out entrance [9]. In the formation of the submerged jump, an abrupt flow transition from supercritical upstream to subcritical downstream may occurs because of air entrainments of the turbulent flow, with the aerated water breaking and spreading [10,11]. On the contrary, for a very large relative drop if the water discharge just larger than trivially small flows, the falling jet will impinge directly on the manhole opposite side wall [12]. It means the flow pattern appears as Regime R3, skipping the Regime R1 and R2. With an ample air supply, a water curtain formed at impingement slides along the manhole inner periphery at a slow rate. Its corresponding outflow spreading through the curtain may has a free surface.

With a limited air supply and bigger falling velocities of the jet, however, a flow rolling motion may appears as a vertical water fountain or a horizontal roller at the impact location to allows air moving into the drop manhole. The air entrainment mechanism under this operation condition is quite similar as that in a hydraulic jump. With the increasement of flow discharge rate, the geyser-like aerated flow propagates up and down inside the drop manhole, leading a choking condition of the manhole system, running full eventually without any interference [13]. The water discharge capacity of the manhole is thereby severely limited by these complicated hydraulic transfer processes downstream the manhole system.

As stated previously, the occurrence of hydraulic jumps mixed with air entrainments shows potential dangers in transitions of the flow inside a drop manhole system. The evaluation of tailwater effects and the prediction of choking conditions are considered as linchpins to ensure the water-carrying capacity of a circular drop manhole. In the present study, a novel classification of flow stages revealing water conveyance capacity took mainly account into experimental observations on tailwater pressures and air suctions.A series of experiments with different drop heights were performed under different operation conditions to investigate the discharge capacity of the manhole under the basic hydraulic

stages. Water levels inside the manhole were analyzed and the corresponding predictive relationships were proposed in a dimensionless form.

2. Methodology

2.1. Flow Stages

For a systematical study, hydraulic stages inside the drop manhole especially which near the downstream sewer invert should be classified primarily. The landmark downstream flow stages of hydraulic transitions were herein grouped into the following four categories:

- Stage S1 (Figure 1a). For small discharges without tailwater effects, the outflow shows a free surface condition. The surface of the flow inside the manhole may waves or rolls slightly with small bubbles from the outlet entrance while no apparent suction of air could be observed;
- Stage S2 (Figure 1b). Due to the backwater pressure, a repelled hydraulic jump forms inside the outlet pipe, then moves towards the manhole outlet entrance, finally behaves as a submerged jump. For small discharges, air bubbles inside the plug flow rise and break from the outlet pipe to the flow surface;
- Stage S3 (Figure 1c). For the full pipe discharge without the tailwater effect, the falling jet starts to suck the air from an air core appearing at the impact location, then rolls violently inside the manhole. Air bubbles are mixed with the high degree of turbulence in the rolling region, resulting in complicated flow patterns, swirling water-wings with its surface atomization for instance;
- Stage S4 (Figure 1d). For the full pipe discharge without backwater pressures but with limited air supply, the outflow changes from air-mixed free surface to pressurized conditions abruptly with bursts of air. Due to an imbalance between the limited air supply and unmet air demand of the falling jet as well as the development of moving hydraulic jumps, the aerated flow erupts inside the manhole, rolling and spreading violently like a geyser.

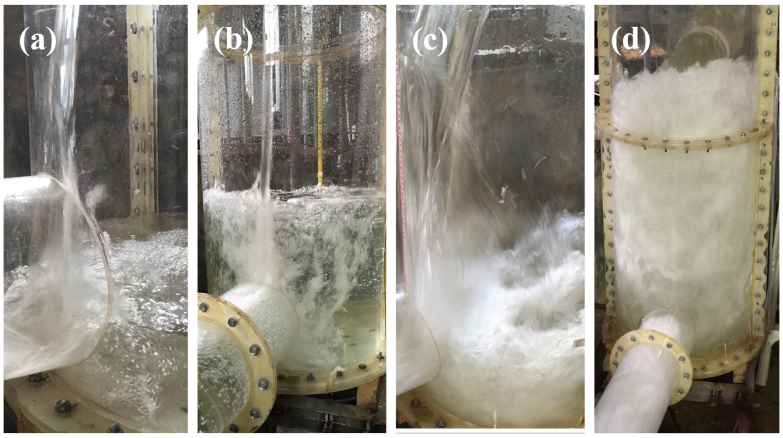

Figure 1. Downstream hydraulic stages: (**a**) S1, (**b**) S2, (**c**) S3 and (**d**) S4.

Operation conditions and characteristics are listed in Table 1. Moreover, different hydraulic transfer processes covering common types of downstream flow patterns could be marked with above basic flow stages:

- S1–S2. For a small discharge, the downstream flow pattern transfers from the free surface to the submerged outflow until running full in the manhole with an addition of the tailwater pressure;
- S1–S3–S4. As the approaching flow rate y_0/D_{in} increases (y_0 = flow filling ratio; D_{in} = inlet pipe diameter), the flow pattern inside a drop manhole transfers from stage S1 to S3. When the water-carrying section reaches the maximum area in the inlet pipe, the downstream flow pattern transfers from stage S3 to S4 with the increase of

approaching velocity. The latter hydraulic transition also ends with a total blockage of the manhole;

- S2 and S4. For a large discharge, the downstream flow pattern affected by tailwater pressures lies somewhere between stage S2 and S4.

Table 1. Characteristics of the novel classification of flow stages.

Stages	Inflow	Outflow	Tailwater	Air Entrainment	Impact
S1	Free surface	Free surface	No	Surface waves	R1, R2, R3a
S2	Free surface	Constrained	Yes	Bubbles from outlet	R1, R2, R3
S3	Full pipe	Free surface	No	Air-mixed rollers	R2c, R3
S4	Full pipe	Aerated	No	Bursts of aerated flow	R3

2.2. Experimental Setup

A schematical layout of the circular drop manhole system is shown in Figure 2a [7]. The experimental facility (see Figure 2b) consisted of an upstream inlet pipe, a circular manhole model and an outlet pipe discharging to a downstream pool. The pool could be considered as a backwater pressurized system by increasing the tailwater depth. The manhole model was represented as a PVC vertical pipe of diameter D_M = 0.54 m with manhole drop height s = 0.93, 1.50 and 2.40 m. It's noteworthy that the sizes of models were chosen to be approach to the prototype to minimize the scale effects. Manhole models were connected to two horizontal plexiglass inlet and outlet pipes of diameter $D_{in} = D_{out}$ = 200 mm with flat bottom junctions. The air demand of the plunging jet was supplied only through a 50 mm-diameter pipe on the top of the manhole model.

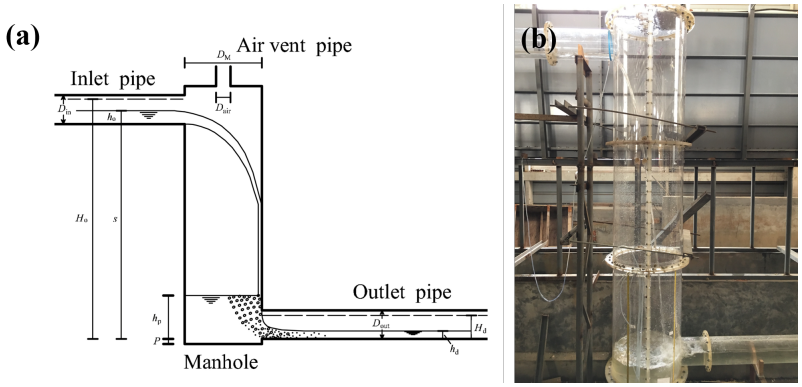

Figure 2. (**a**) Definition sketch for circular drop manhole [7] and (**b**) experimental facility.

Volumetric flow rates (Q) up to 80 L/s could be pumped from a pump and measured in the inflow line using an ultrasonic flowmeter. One piezometer in the upstream, 1.2 m away from the manhole inlet entrance, was used to obtain pressure readings. The downstream flow depth was also measured by a piezometer, which was placed 2 m from the manhole outlet. The time-average water level inside the manhole was measured with a set of piezometers connected to manhole bottom and point gauges of ±0.5 mm reading accuracies.

Seven series of experiments were conducted to investigate the water conveyance capacity as well as corresponding characteristics of downstream hydraulic transition processes in circular drop manholes under different inflow and outflow conditions. Series 1–3 were designed to assess the effect of manhole drop heights on hydraulic performances when both the inflow and outflow were free. By increasing the tailwater depth in the downstream pool, series 4–6 with different drop heights were run under constrained outflow conditions. Note that the lowest tailwater depth in the downstream pool was set to the value where a submerged hydraulic jump or a critical jump would occur. Series 7 was operated for a very large discharge and limited air supply to produce an extreme choking

phenomenon near the exit entrance of manhole. The geometrical characteristics of manhole models and the targeted flow stages in experimental tests are summarized in Table 2.

Table 2. List of experiments.

Series	Drop Heights (m)	Inflow Conditions	Outflow Conditions	Stages
1	2.40	Free surface	Free surface	S1
2	1.50	Free surface	Free surface	S1
3	0.93	Free surface	Free surface	S1
4	2.40	Free surface	Constrained	S2
5	1.50	Free surface	Constrained	S2
6	0.93	Free surface	Constrained	S2
7	0.93	Full pipe	Free to aerated	S3–S4

3. Results

3.1. Dimensionless Water Level versus the Drop Parameter

The average water level inside a drop manhole h_p is one of the main hydraulic characteristics to reveal the water discharge status visually. Under free inflow and outflow conditions (stage S1), Christodoulou [1] found that the ratio of the manhole water level to the drop height h_p/s decreases rapidly with an increasing drop parameter $D = \sqrt{gs}/V_0$ in the range $0 < D < 1.5$, where V_0 is the velocity of the approaching flow, g is the acceleration of gravity. Based on the experimental data, plots of h_p/s versus D at different flow stages are presented in Figure 3.

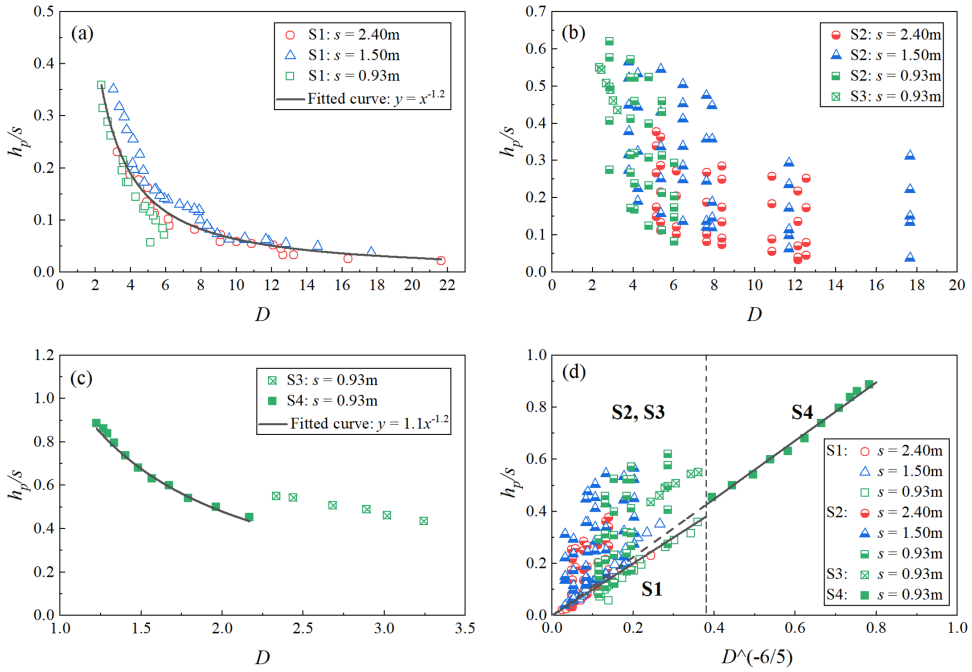

Figure 3. Dimensionless water level versus drop parameter at: (**a**)stage S1; (**b**) stage S2 and stage S3; (**c**) stage from S3 to S4; (**d**) all transition processes.

For stage S1: Figure 3a shows that the experimental data is well fitted by the following empirical equation when both the inflow and outflow conditions are free:

$$\frac{h_p}{s} = D^{-1.2}, \tag{1}$$

Equation (1) indicates that the dimensionless water level h_p/s is solely depends on the drop parameter D in stage S1 for typical manholes($D_{in} = D_{out} \cong 200$ mm, $D_M \cong 0.5$ m). It

further proves that the manhole filling ratio is reduced as the drop height becoming larger at stage S1.

For stage S2, affected by the manual controlled tailwater pressure, the water filling ratio increases rapidly, up to 62% of the drop height in the present experiments. With a constant inflow velocity in a certain drop manhole.the water level at stage S2 is larger than that at stage S1, by approximate two to eight times for typical manholes and tailwater depths in the present study (see Figure 3b).

For the stage S3,the manhole water filling ratio increases slowly with the decrease of the drop parameter. When the flow pattern transforms from stage S3 to stage S4, however, the water level parameter drops abruptly when $D \cong 2.2$ then increases with the growth of the drop parameter. The manhole filling rate augments with the velocity of approaching flow for stage S4. Timely measurements should be taken when the abrupt transition occurs, otherwise leading a fully choking condition inside the manhole (see Figure 3c).

The downstream hydraulic transition processes are well depicted by the dispersion of the stage limits in Figure 3d. One may further notice that the water depth of the flow inside the typical manholes at stage S4 shows a similar trend as that at stage S1 but with a faster filling ratio, given by:

$$\frac{h_p}{s} = 1.1D^{-1.2}, \tag{2}$$

For each drop height with a constant approaching flow velocity, the hydraulic transition from the stage S1 to stage S2 is accompanied with a significantly raising of the water level inside the manhole; The transition from stage S1 to S3 is sharper because the aerated water at S3 is choppier than the submerged flow at S2. For the choking process from stage S3 to S4, the manhole water level falls suddenly then increases in a typical manhole, corresponding to a rapid hydraulic transformation.

3.2. Relative Water Level versus Capacity Froude Number

The capacity of water conveyance in three hydraulic transition processes was assessed from quantification with another important parameter, the dimensionless discharge rate $Q^* = Q/\sqrt{gD_{in}^5}$. This parameter is also known as the pipe Froude number or the capacity Froude number, where Q is the volumetric flow rate. Considering the manhole water level has also to be predicted for a given discharge because of undesired tailwater effects in engineering applications, we adopt another dimensionless parameter h_p/D_{out} with a constant D_{out} in this section. For each flow stage, the relationship between dimensionless parameters h_p/D_{out} and Q^* is depicted in Figure 4.

For stage S1, the experimental data analysis for a given diameter ratio of $D_M/D_{in} = D_M/D_{out} = 2.7$ with a range drop ratio $1.7 < s/D_M < 4.4$ leads an empirical equation to predict (see Figure 4a), given by

$$\frac{h_p}{D_{out}} = \frac{D_M}{D_{out}} Q^{*0.8} + 0.25, \tag{3}$$

For the stage S2, the water level inside the manhole depends entirely on the manual controlled tailwater pressures with a given water discharge rate (see Figure 4b). It indicates that the water carrying capacity of a manhole could be severely restricted with a risk of the high-water-level by tailwater effects.

When it comes to the stage S3, the experimental evidence demonstrates almost the same trend of water level evolution as that at stage S1 (see Figure 4c). In other words, the water conveyance capacity of the manhole will not change too much in the hydraulic transition process from the stage S1 to S3 although the plunging flow becomes more turbulent.

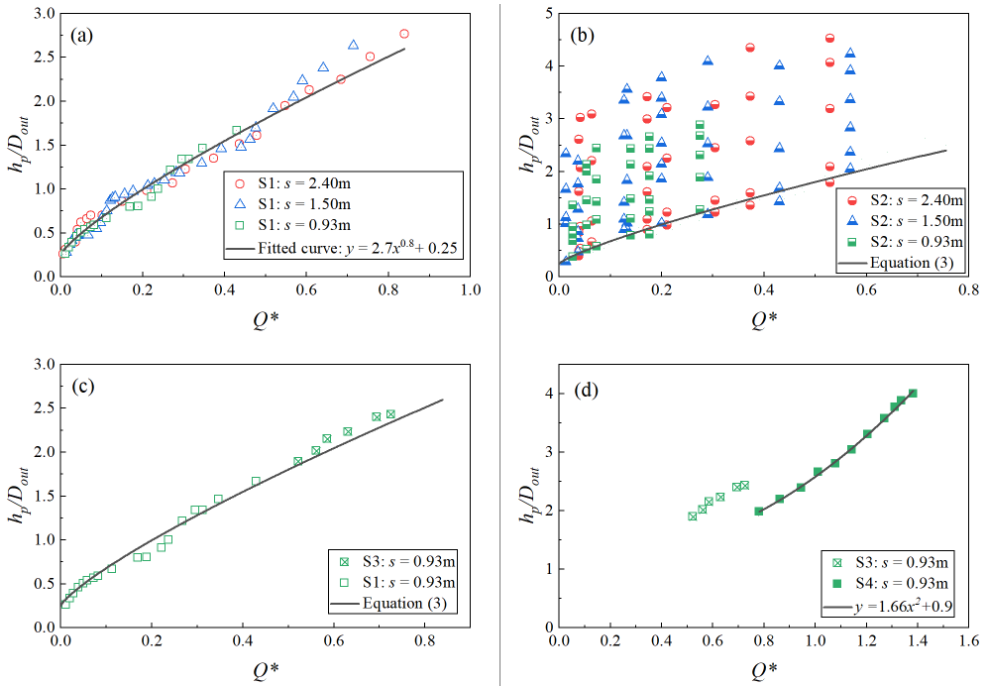

Figure 4. Dimensionless water level versus drop parameter at: (**a**)stage S1; (**b**) stage S2 ; (**c**) stage from S1 to S3; (**d**) stage S3 and S4.

When the aerated flow inside the manhole transfers from the stage S3 into S4, the water level drops abruptly at the onset of S4, then with a faster water filling ratio inside the manhole (see Figure 4d). It means that for a constant discharge rate, the flow inside a drop manhole is considered to reach its discharge capacity when the fully aerated flow is visible in the beginning of the stage S4. Energy considerations for the stage S4 lead to

$$\frac{h_p}{D_{out}} = 1.66Q^{*2} + 0.9, \tag{4}$$

4. Discussion

4.1. Reliability of Formulations

In all experiments of the two-phase flow, the model scale effects on air entrainment processes cannot be completely avoided. First, The air bubbles and turbulent structures in the prototype are very hard to be reproduced in the model scale. Besides, the Reynolds number affects the turbulence at the model scale. The reproduced Weber number also influences the effects of the surface tension. Therefore, it's necessary to assess the reliability of the empirical formulations. In other words, prove that the propsed Equations (1)–(4) for different flow stages can also be used for other manhole diameters.

As is seen in Figure 5, Equation (1) agrees well with Christodoulou's [1] experimental results when the sewer pipes are horizontal (slope k = 0%) and parallel (angle ϕ = 180°), extending the range of agreement. It means that the formulations proposed at the Stage S1 can also be used for other manhole model diameters under free-surface conduit conditions.Thus, the reliability of Equations (1) and (3) have been proved. However, there is no information to further assess the ubiquity and universal capacities of Equations (2) and (4) for Stage S4 due to the lack of comparative data. The coefficient in Equations (2) and (4) may change with various diameters of air vents and manhole models.

4.2. Comparison between Regimes and Stages

As is seen in Table 1, the classic flow regimes (R1, R2 and R3) and our novel hydraulic states (S1, S2, S3 and S4) are totally mixed. Thus, the empirical formulations fitted for different hydraulic stages could not be used directly to predict the characteristics of different

flow regimes without detailed comparisons, and vice versa. Experimental observations support that there should be an abrupt fall of the manhole water level in the stage S3-to-S4 transformation. This special phenomenon could be a marker for the choking occurrence in circular drop manholes. Take a series of Granta's experimental test with D_M = 1.0 m, D_{out} = 0.2 m and s = 1.5 m for example [4]. If the manhole operates under Regime R3 with the orifice outflow, the sudden drop of the water level appearing at $h_p/D_{out} > 1.3$ indicates that the flow patterns is at stage S4. An empirical equation for Regime R3 was proposed by Granta, given by

$$\frac{h_p}{D_{out}} = (7.3 - \frac{D_M}{D_{out}})Q^{*2} + 0.6, \quad (5)$$

The comparison between our Equation (4) for stage S4 and Granta's Equation (5) for Regime R3 is depicted in Figure 6. Apparently, Equation (4) agrees better with the test data. The comparison demonstrates that the relative manhole water level h_p/D_{out} may depends only on the discharge rate Q^*, yet not on the diameter ratio D_M/D_{out} in Regime R3 in this case.

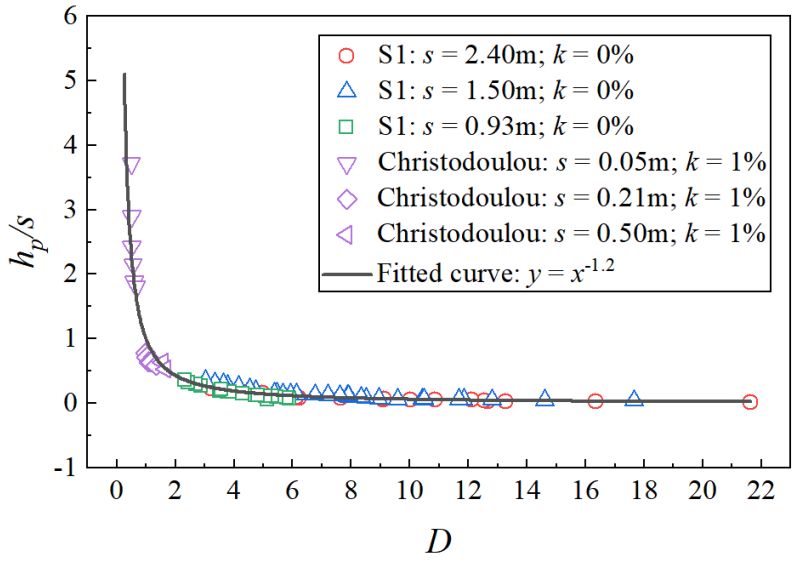

Figure 5. Dimensionless water level versus drop parameter for D_M = 0.05 m, 0.21 m and 0.50 m.

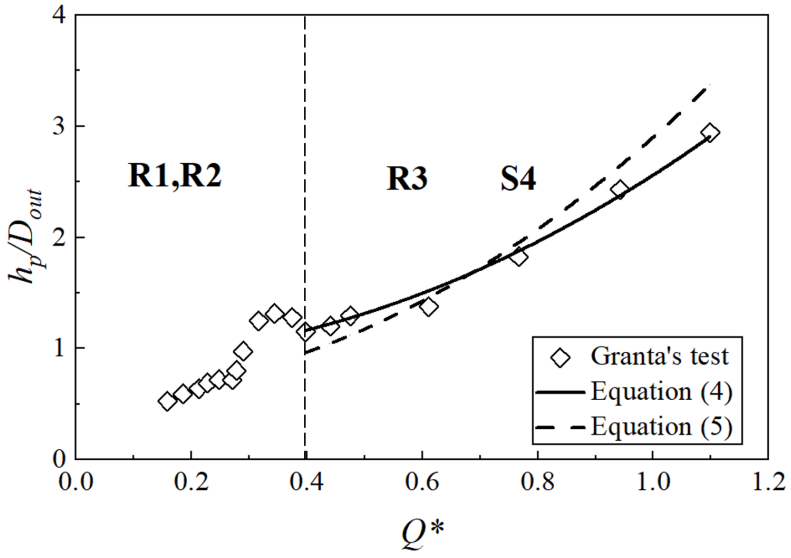

Figure 6. Dimensionless water level versus discharge for D_M =1.0 m, D_{out} = 0.2 m, s =1.5 m and jet opening plate of 40%.

4.3. Prediction of Choking Conditions

The "abrupt-fall" phenomenon observed in the S3–S4 transition and empirical equations for novel regimes proposed in the present work provide an easier way to predict and assess choking risks of drop manholes. Based on traditional regime classification [4], the approaching flow filling ratio $y_0 = h_0/D$ and the capacity Froude number should be determined first. Then evaluate the relative water level h_p/D_{out} and the Froude number for choking inception F_{och}. Finally compare the combined parameter $\psi' = y_0[F_{och} - h_p/D_{out}]$ with $\psi_{ch} = -5.9y_0 + 3.5$ to judge the verification of manhole safety. However, this strategy does not work in some aerated conditions due to the definition of choking occurrences. In terms of the present downstream hydraulic transition studies, Equations (1)–(4) could be used to calculate and predict the domain hydraulic features once the choking of aerated flow occurs with the abrupt fall of the manhole water level. The visual phenomenon in the dimensionless parameters analysis allows to verify the choking risk of a downstream sewer in an easier way. It is a more effective method to define the choking onset according to the abrupt transformation from stage S3 to S4 in the absence of air supply.

5. Conclusions

Circular drop manholes are widely used in urban drainage system for stormwater catchments. The water conveyance capacity of a manhole will be severely restricted , if the downstream flow is affected by backwater pressure or choked with air bursts. This research details the experimental investigation of downstream flow patterns and corresponding hydraulic transitions along with the data analysis. The main conclusions are as following:

- A novel classification of downstream flow patterns consisted of four basic hydraulic stages (i.e., stage S1 to S4) was introduced. Both tailwater pressures and the aeration balance were considered in this classification;
- Three types of hydraulic transitions corresponding to four basic hydraulic stages cover the most common types of hydraulic stages inside circular drop manholes. The changes of water conveyance capacity during these transitions were analyzed with two pairs of dimensionless parameters: dimensionless water level versus drop parameter and relative water level versus capacity Froude number;
- For stages S1 and S4, the ratio of water depths inside the manhole to the drop heights is solely dependent on a dimensionless drop parameter expressed in terms of drop height and the inflow velocity;
- For stages S1 and S3, the capacity Froude number, which reflects the discharge capacity of a manhole system, can be expressed as a function of the drop parameter and the outlet to manhole diameter ratio;
- From stage S1 to S2, with the increase of tailwater pressure, the water level filling ratio increases rapidly up to 62% of the drop height, which points out the high risk of backwater effect;
- From stage S3 to S4, a sudden fall of water level occurs, implying the flow inside a drop manhole will reach its discharge capacity when the fully aerated flow is visible in the beginning of the stage S4;
- Four empirical equations in terms of manhole water filling ratio and discharge are proposed for a further prediction of choking risk.

The experimental results along with the data analysis motivate a novel classification of flow stages. To identify the flow stages, relationships are proposed as a function of dimensionless parameters: the drop parameter, pipe Froude number and diameter ratio for given drop heights. The empirical formulations are intended to be useful to infer either the dimensionless drop height or relative water depth. In the further research, the developed classifications and equations should be proved applicable in practice.

Author Contributions: Conceptualization, C.Z. and F.Z.; writing—original draft preparation, C.Z.; writing—review and editing, F.Z.; supervision, G.Y.; validation, X.S. All authors have read and agreed to the published version of the manuscript.

Funding: This research was funded by China Scholarship Council OF FUNDER grant number 201906710153.

Institutional Review Board Statement: Not applicable.

Informed Consent Statement: Not applicable.

Data Availability Statement: Not applicable.

Acknowledgments: The administrative support of Clara Velte and Preben Buchhave should be acknowledged.

Conflicts of Interest: The authors declare no conflict of interest.

Abbreviations

Lists of symbols:

D_{in}	inlet pipe diameter
D_{out}	outlet pipe diameter
D_M	manhole diameter
g	acceleration of gravity
s	drop height, i.e., distance between inlet and outlet invert elevations
k	inlet pipe angle with respect to the vertical line
ϕ	inlet pipe angle with respect to the outlet pipe
V_0	velocity of the approaching flow
D	drop parameter $=\sqrt{gs}/V_0$
Q	volumetric flow rate
Q^*	capacity Froude number $= Q/\sqrt{gD_{in}^5}$
y_0	flow filling ratio $= h_0/D_{in}$
F_{och}	capacity Froude number for choking incipient

References

1. Christodoulou, G.C. Drop manholes in supercritical pipelines. *J. Irrig. Drain. Eng.* **1991**, *117*, 37–47. [CrossRef]
2. Chanson, H. Hydraulics of large culvert beneath Roman aqueduct of Nımes. *J. Irrig. Drain. Eng.* **2002**, *128*, 326–330. [CrossRef]
3. Chanson, H. Hydraulics of rectangular dropshafts. *J. Irrig. Drain. Eng.* **2004**, *130*, 523–529. [CrossRef]
4. Granata, F.; Hager, G.; Darga, W.H. Hydraulics of circular drop manholes. *J. Irrig. Drain. Eng.* **2011**, *137*, 102–111. [CrossRef]
5. Ma, Y.; Zhu, D.Z.; Rajaratnam, N.; van Duin, B. Energy dissipation in circular drop manholes. *J. Irrig. Drain. Eng.* **2017**, *143*, 04017047. [CrossRef]
6. Fereshtehpour, M.; Chamani, M.R. Flow characteristics of a drop Manhole with an internal ganging baffle Wall in a storm drainage system: Numerical and experimental modeling. *J. Irrig. Drain. Eng.* **2020**, *146*, 04020022. [CrossRef]
7. Zheng, F.; Li, Y.; Zhao, J.; An, J. Energy dissipation in circular drop manholes under different outflow conditions. *Water* **2017**, *9*, 752. [CrossRef]
8. Granata, F.; de Marinis, G.; Gargano, R. Air-water flows in circular drop manholes. *Urban Water J.* **2015**, *12*, 477–487. [CrossRef]
9. Sharif, M.; Kabiri-Samani, A. Flow regimes at grid drop-type dissipators caused by changes in tail-water depth. *J. Hydraul. Res.* **2018**, *56*, 1–12. [CrossRef]
10. Gargano, R.; Hager, M.W.H. Supercritical flow across sewer manholes. *J. Hydraul. Eng.* **2002**, *128*, 1014–1017. [CrossRef]
11. Martino, F.D.; Gisonni, C.; Hager, W.H. Drop in combined sewer manhole for supercritical flow. *J. Irrig. Drain. Eng.* **2002**, *128*, 397–400. [CrossRef]
12. Rajaratnam, N.; Mainali, A.; Hsung, C.Y. Observations on flow in vertical dropshafts in urban drainage systems. *J. Environ. Eng.* **1997**, *123*, 486–491. [CrossRef]
13. Camino, G.A.; Rajaratnam, N.; Zhu, D.Z. Choking conditions inside plunging flow dropshafts. *Can. J. Civil. Eng.* **2014**, *41*, 624–632. [CrossRef]